T. Magn. Soc. Jpn. (Special Issues)., **3**, 12-18 (2019)

<Paper>

Local strain dependence of uniaxial magnetic anisotropy in M–type ferrites

J. Inoue[*,**], H. Nakamura[***], and H. Yanagihara[*]

[*]Institute of Applied Physics, University of Tsukuba, *Tsukuba 305-8573, Japan*

[**]Department of Applied Physics, Tohoku University, *Sendai 980-8577, Japan*

[***] Department of Materials Science and Engineering, Kyoto University, *Kyoto 606-8501, Japan*

We study the magnetic anisotropy (MA) of magnetoplumbite (M)–type ferrites by calculating the electronic structure of clusters formed with an Fe^{3+} ion and O^{2-} ions. Spin–orbit interaction (*LS* coupling) is taken into account. It is shown that the *p–d* mixing between the Fe and O ions and local lattice distortion are crucial to understand the MA of M–type ferrites. Calculations of MA for M–type ferrites doped with Fe^{2+} or Co^{2+} ions demonstrate the importance of local lattice distortion on MA. It is shown that Fe^{2+} ions doped into 2a–site produce metamagnetic character when a compressive deformation along *c*–axis is introduced. It is also shown that the Co^{2+} ions doped onto $4f_1$ site may enhance the uniaxial MA when a compressive deformation is introduced.

Key words : hexagonal ferrite, uniaxial magnetic anisotropy, local lattice distortion, cluster model

1. Introduction

Development of high performance permanent magnets is one of the important technological challenges for the energy-conserving society. Hexagonal ferrite magnets [1),2)] are used most widely on a commercial basis. Even a 10 percent increase in the performance of ferrite magnets makes a great contribution towards energy–saving. It was recently found that doping of divalent Co ions into magnetoplumbite (M)–type ferrites increases magnetic anisotropy (MA).[3)–5)] However, relation between the increase in MA and preferential sites for Co^{2+} ions has not been clarified [6)–9)] and hence, no systematic development of high–performance ferrite magnets has been successful.

Requirements for large MA in permanent magnets are large value of magnetization, strong spin–orbit interaction (SOI), and low crystal symmetry. It is well known that rare–earth Fe (Co) compounds have tetragonal or hexagonal lattice symmetry. Recently, it was reported that thin films of tetragonally distorted spinel ferrites, $Fe(Fe\text{-}Co)_2O_4$, on suitable substrates produce extremely high uniaxial MA.[10)] The mechanism of this high MA has been elucidated by both a phenomenological theory and an electron theory for an octahedral cluster containing a single Co ion and surrounding six O ions.[11),12)]

M–type ferrites, $AFe_{12}O_{19}$ with A = Ba, Sr, or La, have a hexagonal lattice structure and their unit cell contains two formula units (fu's).[1),2)] There are five nonequivalent sites for Fe ions called 2a, 2b, $4f_1$, $4f_2$, and 12k sites. Fe ions are trivalent in M–type ferrites with divalent A (Ba^{2+} and Sr^{2+}) ion. On the other hand, one Fe ion in $LaFe_{12}O_{19}$ is divalent because La ions are trivalent. Magnetic moments of Fe ions at 2a, 2b, and 12k sites are parallel to the bulk moment, while those at $4f_1$ and $4f_2$ sites are antiparallel to the bulk moment. An important point is the shape of the clusters formed by a single Fe ion and surrounding O ions. Clusters for 2a–, $4f_2$–, and 12k–Fe ions are of six–coordinate (octahedral), and the clusters for 2b– and $4f_1$–Fe ions are of five–coordinate (hexahedral) and four–coordinate (tetrahedral), respectively, as shown in Fig. 1. It is noted that the octahedral and tetrahedral clusters are slightly distorted compared to the regular clusters existing in a cubic spinel ferrite.

In this work, using the electron theory for Fe–O clusters with SOI (*LS* coupling), we will show that the small lattice distortion of the clusters is crucial to the magnitude of MA in M–type ferrites and that the MA produced by Co^{2+} ions doped into M–type ferrite is also affected by the cluster distortion. To begin with, we first explain how the trivalent Fe ions produce MA of M–type ferrites in the present cluster model. This is nontrivial because $3d^5$ electron configuration of Fe^{3+} gives rise to null orbital angular momentum resulting in no *LS* coupling. We show that the *p–d* mixing of wave functions on O and Fe ions is essential to understand the MA in oxide magnets.

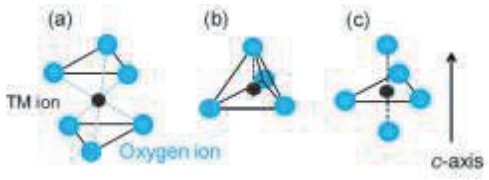

Fig. 1 Types of clusters formed by a TM ion (Fe or Co) and surrounding O ions. (a) Six–coordinate (octahedral) cluster, (b) four–coordinate (tetrahedral) cluster, and (c) five–fold (hexahedral) cluster. Direction of *c*–axis of the M–type ferrite is shown by an arrow.

In next section we explain a model (cluster model) for the electron theory to calculate MA. In section III, we will provide the calculated results of MA for undoped M–type ferrites, followed by those produced for Fe^{2+} and Co^{2+} ions in M–type ferrites. To clarify the effect of cluster distortion on MA of doped ferrites, the MA energy is calculated as a function of cluster distortion. Implications of the calculated results will be discussed, and conclusions are given in section IV.

2. Method of calculation

We perform numerical calculations for clusters with a single Fe^{3+}, Fe^{2+}, or Co^{2+} ion surrounded by six (octahedral cluster), five (hexahedral cluster), and four (tetrahedral cluster) O^{2-} ions using full orbital tight–binding (TB) model with SOI (*LS* coupling) on Fe and Co ions. The 3d–orbitals of the transition metal (TM) ions are spin–polarized and the ions have local moments. The clusters are simplified ones but satisfy the local symmetry.

Parameters of the inter–site *p–d* hopping between five 3d–orbitals on a TM ion and three 2p–orbitals on oxygen ions are determined from Harrison's textbook.[13),14)] Inter–site *p–p* hopping between O ions is also taken into consideration. The atomic energy levels of 2p– and 3d–orbitals and the magnitude of the exchange splitting are fixed by considering the results of the electronic states of the spinel ferrites calculated using first–principles.[15), 16)] Number of electrons on 3d states of Fe^{3+}, Fe^{2+}, and Co^{2+} are five, six, and seven per ion, respectively, and that of O^{2-} is six per ion. The ground state energy is calculated by diagonalizing the Hamiltonian matrix as a function of magnetization direction. It is noted that the mixing of p– and d–orbitals reproduces the correct symmetry–dependence of energy levels as in the crystal field potentials.

The values of the SOI of Fe^{3+}, Fe^{2+}, and Co^{2+} ions are fixed as 0.057, 0.050, and 0.063 eV per ion, respectively.[17)] The values are consistent with the dependence of SOI on Zr^3, where Z and r are the atomic number and ionic radius of the TM ion, respectively.

In the following, "positive uniaxial MA" of the cluster is defined in such a way that the easy–direction of the cluster magnetization coincides with the *c*–axis shown in Fig. 1.

3. Calculated results and discussions

3.1 Magnetic anisotropy of $AFe_{12}O_{19}$

Figure 2 shows the calculated results of MA energy (K_u) for each cluster in M–type ferrites with A = Ba, Sr, and La. Positive K_u indicates the uniaxial MA. The shapes of the clusters used in the calculations are the same as those in the lattices observed for A = Ba, Sr, and La.[18)–20)] Two sets of parameter values are used, among which, one includes no *p–p* hopping and the other includes *p–p* hopping with a weighing factor of 0.5. Although the La–ferrite includes one Fe^{2+} ion in fu because La ion is trivalent, we neglected the existence of Fe^{2+} assuming that all the Fe ions are trivalent, in order to study the dependence of K_u on the small local lattice distortion

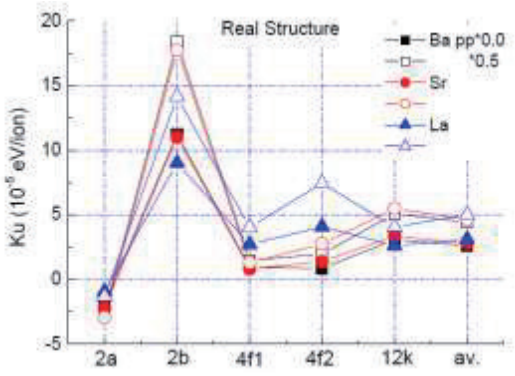

Fig. 2 Calculated results of MA energy, K_u for Fe^{3+} on each nonequivalent site in M–type ferrites. Closed symbols are for those without *p–p* hopping in the cluster model, and open symbols are for those with *p–p* hopping and a weighing factor of 0.5. "av" indicates the averaged value over the K_u values calculated for five nonequivalent sites. 0.1 meV/ion corresponds to 5.6 Merg/cm^3.

As shown in Fig. 2, the 2b site contributes most dominantly to the uniaxial MA because of its lowest cluster symmetry. Nevertheless, the other sites, especially 12k site, may contribute to the total MA because of the abundance of the 12k site. The tendency has already been discussed,[1)] and is consistent with that obtained in the theoretical analysis using crystal field model [21)] and with that in the first–principle calculations.[22)]

The calculated and experimental results of MA energy per unit volume are presented in Table 1. The calculated results are obtained by summing up the contribution of each cluster. We find that the results are in good agreement with the experimental ones. The result calculated by the first–principles is nearly half of the experimental values.[22)] The tendency observed in our calculation suggests the validity of our cluster model. It is noted that the calculated values shown in Table 1 include the effect of *p–p* hopping and that the inclusion of *p–p* hopping enhances the magnitude of K_u values.

Table 1 Experimental and calculated values of K_u in Merg/cm^3 for A = Ba, Sr, and La. The result calculated using first–principles is also presented. The value of K_u of La–ferrite includes a contribution from Fe^{2+} and is larger than those of Ba– and Sr–ferrites by a factor 1~ 2.

A	Ba	Sr	La
Exp. [23)]	3.25	3.57	–
Present cal.	2.45	2.60	2.81
First–principles [22)]	–	1.8	–

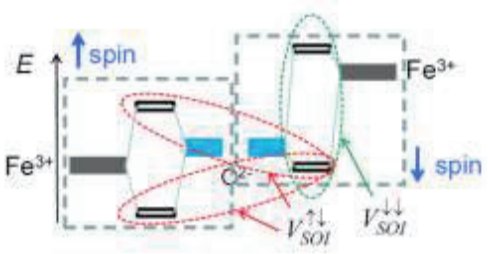

Fig. 3 A schematic diagram of the energy levels of a cluster formed by a TM ion at the center and O ions surrounding the TM ion. Shaded boxes represent the unhybridized levels and open boxes indicate the bonding and antibonding states after p–d mixing. $V_{SOI}{}^{\uparrow\downarrow}$ and $V_{SOI}{}^{\downarrow\downarrow}$ denote up–down spin and down–down spin components of the LS coupling.

To study the effect of the local lattice distortion in $AFe_{12}O_{19}$ on the MA, we performed similar cluster calculations for an ideal M–type ferrite in which the octahedral and tetrahedral clusters are regular octahedrons and tetrahedrons, respectively. The K_u value is 1.6 Merg/cm^3, which is much smaller than those calculated for $AFe_{12}O_{19}$. The result indicates the importance of the local lattice distortion on MA.

The appearance of the MA in Fe^{3+} ions is explained in terms of p–d mixing between the spin–polarized 3d states of an Fe ion and 2p states of O ions. Figure 3 is a schematic presentation of the energy levels for the spin–polarized 3d states and unpolarized 2p states. Shaded boxes represent the energy levels of unhybridized states and white boxes indicate the bonding and antibonding states after p–d mixing. The down–spin bonding states include 3d–orbital components; consequently, the LS coupling becomes active between both up–down and down–down spin components, resulting in a weak MA in Fe^{3+} ions.

Some discussions on the validity of the present calculations are ready. The bulk K_u of Ba–ferrite was calculated to be 0.6 Merg/cm^3 by using the crystal field model,[21] in which the local K_u values were reported to be 17.4 × and –2 ~ 6 $\times 10^{-5}$ eV/ion for 2b–Fe and the other Fe ions, respectively. Although the tendency of the local K_u values agrees with the present results, the bulk K_u is smaller than that in the present model. The result may be attributed to the negative value of local K_u for the abundant 12k–site Fe ions.

The first principles calculation of the local K_u for Sr–ferrite in the Wien2K with GGA+U formalism[22] gives 24 × and –1 ~ 2 × 10^{-5} eV/ion for 2b–Fe and the other Fe ions, respectively. Although the bulk K_u value shown in Table 1 is consistent with the present result, the local K_u values except for 2b–Fe are not necessarily consistent with ours. We attribute the difference to the long–range effect neglected in our cluster model. Resultant numerical error inherent to the present model seems be of the order of 10^{-5} eV/ion, because the accuracy in the numerical calculation is better than 10^{-7} eV/ion.

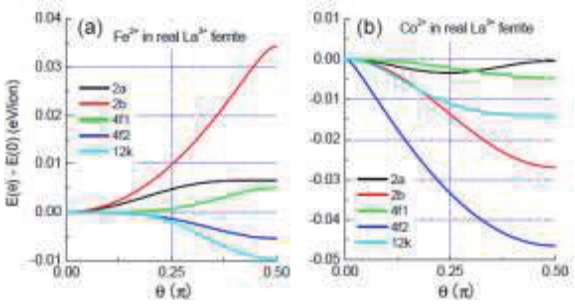

Fig. 4 MA energy, calculated in the cluster model, as a function of angle θ of the magnetization direction measured from c–axis shown in Fig. 1 for (a) Fe^{2+} and (b) Co^{2+} ions in the nonequivalent sites of La–ferrite.

3.2 MA of divalent Fe and Co ions

To clarify the sites occupied by Co^{2+} in M–type ferrites is crucial in the fabrication of high performance ferrite magnets, however, the experimental results are controversial:[6),7),24)–27)] Mössbauer and Raman measurements suggest $4f_2$ site as the occupied site, while Neutron diffraction and Extended X–ray Absorption Fine Structure (EXAFS) measurements suggest $4f_1$ site. As for the occupation of Fe^{2+} ions, on the other hand, both experimental and theoretical results suggest 2a site as the most preferential site.[22),28)] In addition, a metamagnetic transition observed in the magnetization process for Fe^{2+} doped (Ca-La)$Fe_{12}O_{19}$ might be a clue to identify the occupation sites of Fe^{2+} ions.[28)]

To examine the effects of Fe^{2+} and Co^{2+} ions on MA, we perform numerical calculation of MA energy for clusters which contain Fe^{2+} or Co^{2+}. The shape of the cluster is assumed to be the same as that in La–ferrite. Calculated results for Fe^{2+} and Co^{2+} ions as a function of magnetization direction θ, the angle measured from c–axis, are presented in Fig. 4(a) and 4(b), respectively.

As shown in figure 4(a), Fe^{2+} ions on 2a, 2b, and $4f_1$ sites enhance the uniaxial K_u, while those on $4f_2$ and 12k sites suppress it. However, no such tendency has been observed in experiments. Furthermore, the θ–dependence of MA energy on 2a–Fe shows no tendency of a metamagnetic transition. As for Co^{2+} ions in La–ferrite, they, except for those on 2a site, suppress the uniaxial MA as shown in Fig. 4(b). The characteristic feature shown in Fig. 4(b) has been found to be unchanged for Co^{2+} ions doped in the other M–type ferrites. The MA energy thus calculated for Co^{2+} ion doped into any site in M–type ferrites would not explain the observed increase in the uniaxial K_u.

As mentioned, the shape of the clusters used in the calculations is assumed to be the same as that in the lattice structure of La–ferrite. However, in (La-Ca)–ferrite for example, random distribution of Fe^{3+} and Fe^{2+} ions may give rise to additional lattice distor-

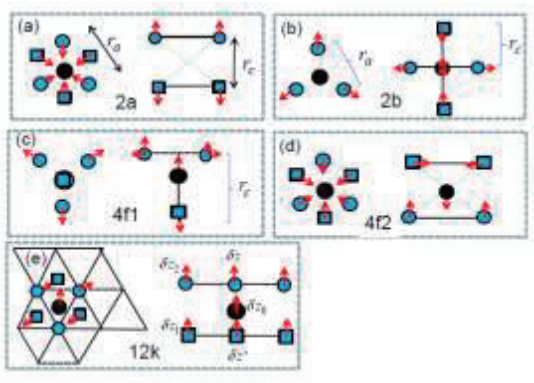

Fig. 5 Types of cluster distortions denoted by the shift (small red arrows) of O and Fe ions for (a) 2a, (b) 2b, (c) $4f_1$, (d) $4f_2$, and (e) 12k sites. Right and left panels of each figure are the projections of the cluster onto the *c*–plane and a plane along the *c*–axis, respectively. Two distances r_a and r_c are defined as the in–plane O–O distance and inter–plane one, respectively.

tion because of different ionic radii between Fe^{3+} and Fe^{2+} ions. Distribution of La and Ca ions may also lead to a similar effect. As shown in the previous subsection, the MA of M–type ferrite is sensitive to the lattice distortion of clusters, and therefore, it is expected that the calculated results shown in Fig. 4 might be altered by lattice distortion of the clusters. In the following, we perform cluster calculations by introducing cluster distortions.

As the details of local lattice distortion in (La-Ca)–ferrite are unknown, we first survey the characteristic feature of the local lattice distortion of Fe–O clusters in Ba–, Sr–, and La–ferrites.[18)–20)] Results are depicted in Fig. 5, where small arrows denote the shifts of O and Fe ions from the potions of ideal clusters. The shifts for 2a–site cluster, for example, are depicted in Fig. 5(a). The left figure is a projection of the cluster on the *c*–plane, and shows that the O ions on both upper and lower triangles shrink, that is, the distance r_a shown in the figure becomes smaller than that of the regular octahedron in the cubic spinel ferrite. The right figure is a projection on to a plane along *c*–axis. It shows that O ions on the upper triangle shift upward and those on the lower triangle shift downward, resulting in an increase in the distance r_c. Figures for the other clusters should be understood similarly, except for the shift of the Fe ions along the *c*–axis. It is notable that result for the 12k–cluster exhibits complicated lattice distortion as depicted in Fig. 5(e).

The O–ion position is shifted from the position of the regular octahedron or tetrahedron by a small amount of (δx_0, δy_0, δz_0), which may be estimated by using the X–ray diffraction data for Ba, Sr, and La–ferrites.[18)–20)] The estimated values are $\delta x_0 = -0.01 \sim 0.015$ Å, $\delta y_0 = -0.02 \sim 0.01$ Å, and $\delta z_0 \lesssim 0.04$ Å for 2a, $4f_1$ and $4f_2$ site clusters. By using these values, the range of r_a and r_c values defined in Fig. 5 have been evaluated.

Table 2. Estimated magnitude of cluster distortion in M–type ferrites, normalized r_c/r_a, and shift of Fe ion $|\delta z|$. Values for 12k–site cluster are omitted because of the complexity of the cluster distortion.

	Normalized r_c/r_a	Shift of Fe ion $\|\delta z\|$ (Å)
2a	1.08 ~ 1.12	0
2b	0.87 ~ 0.90	0.006 ~ 0.007
$4f_1$	1.06 ~ 1.07	0.002 ~ 0.003
$4f_2$	1.10 ~ 1.17	0.009 ~ 0.011
12k	–	–

The cluster distortion may be characterized by two quantities, a ratio r_c/r_a where r_c and r_a are the in–plane and inter–plane distances between two O ions, respectively, and δz is the shift of Fe ion as defined in Fig. 5. Here, we introduce a normalized ratio $(r_c/r_a)_n$ that is the value of r_c/r_a normalized by that for regular octahedron or tetrahedron. The $(r_c/r_a)_n$ value for 2b–site cluster is determined using 2b–site cluster in the ideal M–type ferrite in which regular octahedrons and tetrahedrons are included. Table 2 shows values of normalized ration $(r_c/r_a)_n$ and $|\delta z|$ for clusters with the nonequivalent Fe sites. In the following, we use these values as a measure of lattice distortion to calculate the dependence of K_u on the local lattice distortion in M–type ferrite doped with Fe^{2+} or Co^{2+} ions.

Now, we study the dependence of K_u values on local lattice distortion for Fe^{2+} and Co^{2+} ions doped in Sr–ferrite. We focus our attention on the Fe^{2+} ion on 2a site, which may be responsible for the metamagnetic behavior, and on the Co^{2+} ion on $4f_1$ and $4f_2$ sites, which are suggested to be plausible for Co^{2+} occupation.

Figure 6(a) shows calculated values of K_u of Sr –ferrite in which 20 % Fe^{2+} ions are doped into 2a sites. The range of the lattice distortion is $0.9 < (r_c/r_a)_n < 1.0$ and $-0.01 < \delta z < 0.01$. The value of δz is zero because of the lattice symmetry, however, we have introduced it virtually for comparison with results obtained for the other clusters. The K_u value on Fe^{2+} ion and that of the bulk Sr–ferrite calculated in the previous subsection, have been averaged over. Red region shows positive K_u and blue and green regions indicate negative K_u. The linear dependence of K_u on $(r_c/r_a)_n$ is the same as the tetragonality dependence of K_u given by the relation $K_u = B\,(c/a-1)$ in cubic lattices, where B is the magnetoelastic constant. The dependence of K_u on δz is symmetrical because of the symmetry of the 2a–site cluster along the c–axis.

Because θ–dependence of K_u is given as $K_u \sim K_1 \sin^2\theta + K_2 \sin^4\theta$, several magnetic states may appear depending on the signs and magnitudes of K_1 and K_2. Therefore, we have approximately fitted the calculated results of K_u (θ) using the equation above, and have

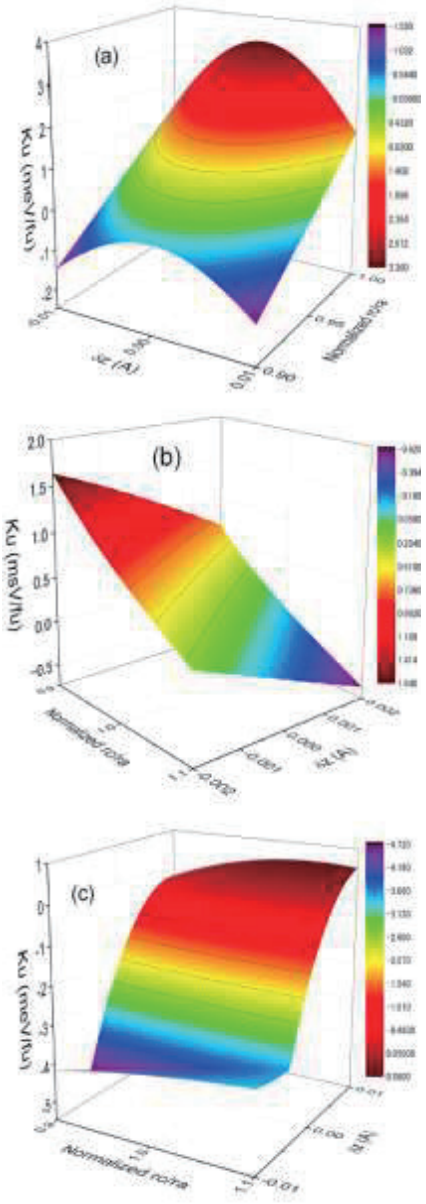

Fig. 6 Calculated results of K_u (in Merg/cm^3) of Sr–ferrite with 20 % doping of Fe^{2+} or Co^{2+} ions. Results are plotted as a function of normalized r_c/r_a ratio, $(r_c/r_a)_n$ (see text), and δz (in Å), which characterize the cluster distortion and the shift of Fe or Co ions. (a) Fe^{2+} doping on 2a site, (b) Co^{2+} doping on $4f_1$ site, and (c) Co^{2+} doping on $4f_2$ site.

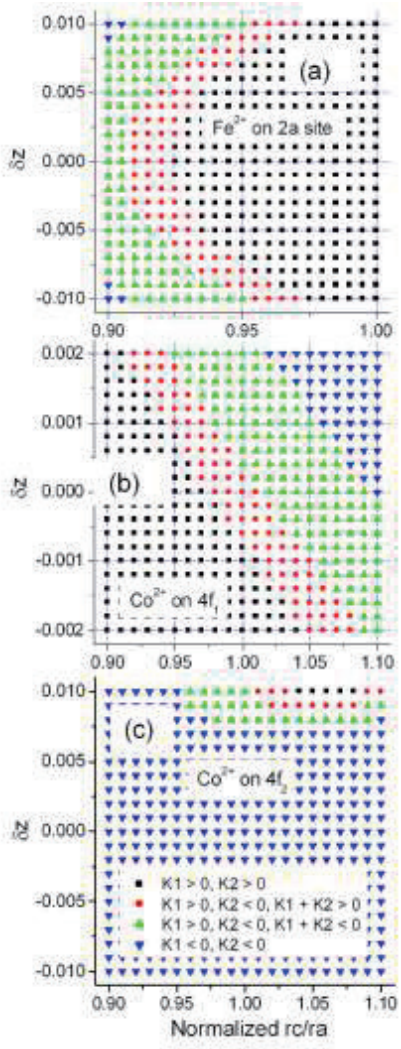

Fig. 7 Signs of K_1, K_2, and K_u calculated as a function of normalized r_c/r_a ratio and δz (in Å) to characterize the magnetic states of Sr–ferrites with 20 % doping of Fe^{2+} or Co^{2+} ions. (a) Fe^{2+} ion on 2a site, (b) Co^{2+} ion on $4f_1$ site, and (c) Co^{2+} ion on $4f_2$ site.

obtained values of K_1 and K_2. These values are useful to semi-quantitatively discuss the dependence of the magnetic state on lattice distortion. Combination of the signs of K_1, K_2, and K_u is plotted in Fig. 7(a) as a function of $(r_c/r_a)_n$ and δz. For $(r_c/r_a)_n > 0.925$ with $\delta z = 0$, all values are positive, while states with $K_1 > 0$, $K_2 < 0$, and $K_u > 0$ appear with decreasing $(r_c/r_a)_n$. In these states the metamagnetic transition may occur when an in–plane external magnetic field is applied. The most notable result shown in Fig. 6(a) and Fig. 7(a) is that the sign of MA is altered by a very small change in the inter–atomic distance.

Figure 6(b) shows the results for K_u of Sr–ferrite with 20 % doping of Co^{2+} on $4f_1$ site. The red and blue regions indicate positive and negative K_u, respectively. The magnitude of the local distortion of the cluster containing $4f_1$ site in the undoped Sr–ferrite corresponds to that in the blue region. With decreasing $(r_c/r_a)_n$, which implies increasing the compression along the c–axis, K_u values increase and become positive as shown in the figure. Similarly, K_u value becomes positive as δz turns to be negative.

Combination of the signs of K_1, K_2, and K_u is plotted in Fig. 7(b) as a function of $(r_c/r_a)_n$ and δz. We find the

blue region with negative K_u changes to be positive with decreasing $(r_c/r_a)_n$. Similar change occurs in case of sign change in δz from positive to negative. We see that the combination of signs of K_1, K_2, and K_u is altered by a few % change in $(r_c/r_a)_n$, as well as by a small shift δz of Co ion.

Similar plots for Sr–ferrite with 20 % doping of Co^{2+} on $4f_2$ site are presented in Fig. 6(c) and Fig. 7(c). It is noted that color presentation in Fig. 6(c) is different from that in figure 6(b): zero of K_u resides in the blue region in Fig. 6(b), while it is in the red region in Fig. 6(c). As shown in Table 2, values of $(r_c/r_a)_n$ and δz for $4f_2$ site cluster in the undoped ferrite are close to 1.1 and –0.01 Å, respectively. Therefore, 20 % doping of Co^{2+} on $4f_2$ site makes K_u strongly negative. The plot in Fig. 7(c) shows that the negative sign of K_u would not be altered by weak distortion of the cluster.

We have thus investigated the overall feature of the effects of the local lattice distortion, that is, the cluster deformation, on K_u values as well as on the signs of K_1, K_2, and K_u. The possible magnitude of the local lattice distortion after Fe^{2+} or Co^{2+} doping was estimated by comparing the distortions in Ba–, Sr–, and La–ferrites with those in the ideal structure. The results may be summarized in the following manner.

Because the MA induced by Fe^{2+} and Co^{2+} ions is much larger than that induced by Fe^{3+} ion, dopant of small amount of Fe^{2+} and Co^{2+} ions may change the character of MA of M–type ferrites. When the lattice structure of doped ferrites is assumed to be the same as that of undoped ferrite, the change in K_u values for Fe^{2+} doping depends on the doped site of Fe^{2+}, while K_u for Co^{2+} ion is negative and independent of the doped site. However, such change in MA of doped ferrites strongly depends on the local lattice distortion, a very small change in $(r_c/r_a)_n$ of the cluster and/or a small shift in the position of Fe^{2+} (Co^{2+}) ions. Furthermore, such MA change depends on the occupation sites. For Fe^{2+}–doped 2a site, the metamagnetic feature appears under cluster compression along the c–axis. For Co^{2+}–doped $4f_1$ site, similar compression makes K_u positive.

The results are consistent with the observed ones, however, several discussions are possible. First, so far no explicit observation for the relation of MA change and local lattice distortion has been reported. Because the lattice distortion introduced in our calculation is very small, high–precision local probe is required to measure the lattice distortion.[30]

Secondly, in our calculations, the distortion of each cluster was treated independently. This treatment may not always be correct. For example, Fe ions on $4f_2$ sites form dumbbell structure in M–type ferrites, that is, two neighboring octahedrons share a triangle face, resulting in a double–cluster structure. It should be noted that, for this type of double–cluster structure, K_u value induced by two Co^{2+} ions depends on the distance between the two Co^{2+} ions. Our preliminary results show that with decreasing distance, direct overlap of 3d–electron clouds increases and contributes to make K_u positive. The tendency is the same with that in the usual hexagonal Co lattices.

Thirdly, we would like to discuss the long–range effects of crystal field potential on K_u values. The bulk K_u values of M–type ferrites doped with 20% Co^{2+} or Fe^{2+} ions are of the order of 1 meV/fu as shown in Fig. 6, which corresponds 0.5^{-3} eV per Co or Fe ion. The long–range effects on the local K_u of Co^{2+} have been investigated in a simple model for tetragonally distorted spinel ferrites in which a local trigonal symmetry around TM ions on the so-called B–site is produced due to characteristic lattice structure in the second nearest neighbor sites.[31] It has been shown that the local trigonal symmetry reduces the K_u value of the tetragonally distorted spinel ferrites.[12] Although M–type ferrites have no such local symmetry, existence of Ba or Sr ions and distribution of Co^{2+} and/or Fe^{2+} ions may reduce the bulk K_u values. Nevertheless, the local K_u values of Co^{2+} and Fe^{2+} remain sufficiently large as compared with those of Fe^{3+}, and therefore the semi-quantitative results shown in Figs. 6 and 7 would be unchanged. It is noted that such effect is not large for Fe^{3+} ions because the up and down spin states are already split by the large exchange field.

Finally, the clusters in ferrites are connected with one another, and therefore, the distortion of each cluster is affected by other clusters. Furthermore, such local lattice distortion is influenced by the distribution of divalent and trivalent ions in the lattice. One possible way to clarify such local lattice distortion in a doped lattice could be the method of lattice relaxation in the first–principles. In this case, however, highly precise calculation is also desirable.

4. Conclusions

We explained the MA of M–type ferrites by calculating the electronic structure of clusters with a single Fe^{3+} ion and surrounding O^{2-} ions. The SOI (*LS* coupling) was introduced in the magnetic ion. We found that the calculated results agree with the experimental ones fairly well, and attributed the mechanism of MA of Fe^{3+} ions to the *p–d* mixing between 2p– and 3d–orbitals of O^{2-} and Fe^{3+} ions, respectively. It was pointed out that a small amount of lattice deformation of the clusters is crucial for quantitative understanding of the MA.

Our cluster calculations showed that MA of M–type ferrites doped with Fe^{2+} or Co^{2+} ions is also strongly affected by a small amount of lattice distortion. It was shown that Fe^{2+} ions doped onto 2a–site produce metamagnetic character when compressive deformation along the c–axis is introduced. It was also shown that the Co^{2+} ions doped onto $4f_1$ site may increase the uniaxial MA when the compressive deformation is introduced.

For material design of ferrite magnets, however, precise measurements of local lattice distortion and

detailed first–principles calculations of MA with local lattice relaxation are required.

Acknowledgements This study was partially supported by the project "High Performance Magnets" of Japan Science and Technology Agency, Japan.

References

1) J. Smit and H. P. J. Wijn, Ferrite, *Philips Technical Library*, Eindhoven (1960).
2) H. Kojima, Ferromagnetic Materials, Vol. **3**, ed. E. P. Wohlfarth, p. 305, (North-Holland, Amsterdam).
3) H. Nishio, K. Iida, Y. Minachi, K. Masuzawa, M. Kawakami, and H. Taguchi, *J. Magn. Soc. Jpn.* **23**, 1097 (1999).
4) Y. Ogata, T. Takami, and Y. Kubota, *J. Jpn. Soc. Powder Metal.* **50**, 636 (2003).
5) Y. Kobayashi, S. Hosokawa, E. Oda, and S. Toyota, *J. Jpn. Soc. Powder Metal.* **55**, 541 (2008).
6) G. Wiesinger, M. Müller, R. Grössinger, M. Pieper, A. Morel, F. Kools, P. Tenaud, J.-M. Le Breton, and J. Kreisel, *phys. stat. sol.* (a) **189**, 499 (2002).
7) A. Morel, J.-M. Le Breton, J. Kreisel, G. Wiesinger, F. Kools, and P. Tenaud, *J. Magn. Magn. Mater.* **242–245**, 1405 (2002).
8) M. Pieper, F. Kools, and A. Morel, Phys. Rev. B **65**, 184402 (2002).
9) Y. Kobayashi, E. Oda, T. Nishiuchi, and T. Nakagawa, *J. Ceram. Soc. Jpn.* **119**, 285 (2011).
10) T. Niizeki, Y. Utsumi, R. Aoyama, H. Yanagihara, J. Inoue, Y. Yamasaki, H. Nakano, K. Koike, and E. Kita, *Appl. Phys. Letters* **103**, 162407 (2013).
11) A. Lisfi, C. M. Williams, L. T. Nguen, J. C. Lodder, A. Coleman, H. Corcoran, A. Johnson, P. Chang, A. Kumar, and W. Morgan, *Phys. Rev. B* **76**, 054405 (2007).
12) J. Inoue, H. Yanagihara, and E. Kita, *Materials Research Express* **1**, 046106 (2014).
13) W. A. Harrison, *Electronic Structure and the Properties of Solid*, 1980 (W. H. Freeman and Company, San Franscisco).
14) J. Inoue, *J. Phys. D: Appl. Phys.* **48**, 445005 (2015).
15) Z. Szotek, W. M. Temmerman, D. Ködderitzsch, A. Svane, L. Petit, and H. Winter, *Phys. Rev. B* **74**, 174431 (2006).
16) T. Kida, S. Honda, H. Itoh, J. Inoue, H. Yanagihara, E. Kita, and K. Mibu, *Phys. Rev. B* **84**, 104407 (2011).
17) F. E Mabbs and D. J. Machin, *Magnetism and Transition Metal Complexes*, 2008 (Dover, New York USA).
18) X. Obradors, X. Solans, A. Collomb, D. Samaras, J. Rodriguez, M. Pernet, and M. Font-Altaba, *J. Solid State Chem.* **72**, 218 (1988).
19) M. V. Cabanas, J. M. Gonzalez Calbet, J. Rodriguez Carvajal, and M. Vallet Regi, *J. Solid State Chem.* **111**, 229 (1994).
20) M. Küpferling, R. Grössinger, M. W. Pieper, G. Wiesinger, H. Michor, C. Ritter, and F. Kubel, *Phys. Rev. B* **73**, 144408 (2006).
21) X. You, G.-J. Yang, D.-P. Chu, and H.-R. Zhai, *phys. stat. sol.* (b) **157**, 685 (1990).
22) V. Chlan, K. Kouřil, K. Uličiná, H. Štěpánková, J. Töpfer, and S. Seifert, *Phys. Rev. B* **92**, 125125 (2015).
23) B. Shirk and W. Buessem, *J. Appl. Phys.* **40**, 1294 (1969).
24) Y. Kobayashi, E. Oda, T. Nakagawa, and T. Nishiuchi, *J. Jpn. Powder Metal.* **63**, 101 (2016).
25) Y. Kobayashi, PhD thesis, Osaka University (2016), [in Japanese].
26) H. Nakamura, *Magnetics Jpn.* **13**, 59 (2018), [in Japanese].
27) Y. Kobayashi, *Magnetics Jpn.* **13**, 68 (2018), [in Japanese].
28) A. Shimoda, K. Takao, K. Uji, T. Waki, Y. Tabata, and H. Nakamura, *J. Solid State Chem.* **239**, 153 (2016).
29) K. Takao, T. Waki, Y. Tabata, K. Uji, and H. Nakamura, to be submitted.
30) H. Nakamura, A. Shimoda, T. Waki, Y. Tanabe, and C. Meny, *J. Phys. Condens. Matter* **28**, 346002 (2016).
31) J. C. Slonczewski, *Phy. Rev.* **110**, 1341 (1958).

Received Oct. 09, 2018; Accepted Dec. 19, 2018